ORIGINAL ARTICLE

Lung Innate Lymphoid Cell Composition Is Altered in Primary Graft Dysfunction

Laurel A. Monticelli[1,2]*, Joshua M. Diamond[3]*, Steven A. Saenz[2‡], Elia D. Tait Wojno[2§], Mary K. Porteous[3], Edward Cantu[4], David Artis[2‖], and Jason D. Christie[3‖¶]

[1]Division of Pulmonary and Critical Care Medicine and [2]Joan and Sanford I. Weill Department of Medicine, Department of Microbiology and Immunology, Jill Roberts Institute for Research in Inflammatory Bowel Disease, Weill Cornell Medicine, Cornell University, New York, New York; and [3]Division of Pulmonary, Allergy, and Critical Care Medicine, and [4]Division of Cardiovascular Surgery, Center for Translational Lung Biology, Perelman School of Medicine, University of Pennsylvania, Philadelphia, Pennsylvania

Abstract

Rationale: Primary graft dysfunction (PGD) is the leading cause of early morbidity and mortality after lung transplantation, but the immunologic mechanisms are poorly understood. Innate lymphoid cells (ILC) are a heterogeneous family of immune cells regulating pathologic inflammation and beneficial tissue repair. However, whether changes in donor-derived lung ILC populations are associated with PGD development has never been examined.

Objectives: To determine whether PGD in chronic obstructive pulmonary disease or interstitial lung disease transplant recipients is associated with alterations in ILC subset composition within the allograft.

Methods: We performed a single-center cohort study of lung transplantation patients with surgical biopsies of donor tissue taken before, and immediately after, allograft reperfusion. Donor immune cells from 18 patients were characterized phenotypically by flow cytometry for single-cell resolution of distinct ILC subsets. Changes

in the percentage of ILC subsets with reperfusion or PGD (grade 3 within 72 h) were assessed.

Measurements and Main Results: Allograft reperfusion resulted in significantly decreased frequencies of natural killer cells and a trend toward reduced ILC populations, regardless of diagnosis (interstitial lung disease or chronic obstructive pulmonary disease). Seven patients developed PGD (38.9%), and PGD development was associated with selective reduction of the ILC2 subset after reperfusion. Conversely, patients without PGD exhibited significantly higher ILC1 frequencies before reperfusion, accompanied by elevated ILC2 frequencies after allograft reperfusion.

Conclusions: The composition of donor ILC subsets is altered after allograft reperfusion and is associated with PGD development, suggesting that ILCs may be involved in regulating lung injury in lung transplant recipients.

Keywords: primary graft dysfunction; lung transplantation; chronic obstructive pulmonary disease; interstitial lung disease; innate immune cell

At a Glance Commentary

Scientific Knowledge on the Subject: Primary graft dysfunction (PGD) is the leading cause of early morbidity and mortality after lung transplantation, but the immunologic mechanisms are poorly understood. Innate lymphoid cells (ILCs) are a heterogeneous family of immune cells regulating pathologic inflammation and beneficial tissue repair. However, whether changes in donor-derived lung ILC populations are associated with PGD development has never been examined.

What This Study Adds to the Field: The composition of donor ILC subsets is altered after allograft reperfusion and is associated with PGD development, suggesting that ILCs may be involved in regulating lung injury in lung transplant recipients.

Primary graft dysfunction (PGD), a form of acute lung injury affecting lung transplant recipients, remains the most important cause of early morbidity and mortality after lung transplant. PGD is believed to predominantly result from severe ischemia–reperfusion injury occurring at the time of the transplant procedure and is characterized by alveolar inflammation and diffuse alveolar damage (1). Although numerous clinical risk factors are proposed to contribute to PGD development (2–4), studies using *in vivo* animal models have also demonstrated an immunologic basis for disease pathogenesis (5). The immune response is characteristically biphasic, consisting of resident donor cells regulating the early phase of lung injury until an influx of recipient host cells mediate the later phase of tissue damage (6, 7). Previous studies have implicated critical roles for donor-derived resident neutrophils, alveolar macrophages, and conventional adaptive lymphocytes in the initial pathogenesis of lung ischemic–reperfusion injury (6–12). However, whether other immune cell subsets may contribute to disease pathogenesis, or conversely may help protect against lung injury, is poorly characterized.

Innate lymphoid cells (ILCs) are an emerging family of immune cells that have been implicated in promoting host metabolism, immunity, inflammation, and tissue repair at multiple barrier surfaces (13–15). Commonly referred to as the innate counterpart to the CD4$^+$ helper T–cell lineage, the ILC family shares morphological, developmental, and functional similarities with CD4$^+$ T cells, but lacks antigen receptors (13, 16–18). However, unlike other innate lymphocytes, such as natural killer (NK) cells, ILCs do not possess cytotoxic function and instead exert their functionality through robust production of cytokines and growth factors. Based on transcription factor expression and cytokine profile, human ILCs fall into three main subsets: group 1 (ILC1s), group 2 (ILC2s), and group 3 (ILC3s). Importantly, alterations in the accumulation or functionality of different ILC subsets have been associated with multiple inflammatory diseases of the respiratory system, including asthma, chronic obstructive pulmonary disease (COPD), and interstitial lung disease (ILD) (13, 19–24). Murine models have demonstrated a critical role for ILC2s in driving pathogenesis of lung inflammation, primarily via IL-5 and IL-13 (25–31). Critically however, ILCs are not always detrimental to the host. Under conditions of severe lung injury, we have demonstrated in murine models that ILC2s are crucial for promoting airway epithelial repair and restoring lung tissue homeostasis through the growth factor amphiregulin (32). Thus, ILCs appear to be important players in the balance between pathologic inflammation versus beneficial tissue repair in the lung, raising the possibility that these immune cells may be involved in PGD development. We therefore performed a cohort study to *1*) evaluate whether the subset composition of lung-resident ILCs changes with allograft reperfusion and *2*) evaluate the association between changes in donor ILC populations and the development of PGD after lung transplantation.

Methods

Subject Selection and Study Design

A single-center cohort study was chosen to minimize the time elapsed between surgical biopsy removal and subsequent tissue processing for isolation of live immune cells. Subjects underwent lung transplantation at the University of Pennsylvania between April 2013 and April 2014 as part of the ongoing multicenter, prospective Lung Transplant Outcomes Group cohort study (*see* Figure E1 in the online supplement for flowchart of patient enrollment). Patients with available surgical biopsies from the allograft before and immediately after reperfusion were eligible for inclusion. Clinical information regarding donor, recipient, and perioperative characteristics and events were prospectively recorded on standardized case report forms, as previously described (3, 33). The Penn institutional review board approved the study, and all study subjects provided written consent.

PGD Definition

PGD cases were defined using the International Society for Heart and Lung Transplantation guidelines, with PGD defined as the presence of diffuse parenchymal infiltrates with aPa_{O_2}:F_{IO_2} ratio less than 200 at any time in the first 72 hours after allograft reperfusion (3, 34–36). Of note, all patients that had PGD grade 3 at 72 hours also had grade 3 PGD present within the first 24 hours. Furthermore, all patients except for one had grade 3 PGD on Postoperative Day 0.

Sample Collection and Cell Isolation

Lung tissue biopsy samples were obtained from the allograft at two time points: *1*) after procurement but before implantation, and *2*) *in situ* from the recipient immediately after allograft reperfusion. All biopsies were obtained from the periphery of the lung, including visceral pleura, routinely in the right middle lobe or left lingula. Central airways were not sampled. Sampling was performed according to a standardized protocol and conducted exclusively by a single surgeon. Tissue biopsies from the allograft measured approximately 0.5 mm in width and 3–4 mm in length. Tissues contained an average of three rows of surgical staples.

After excision, tissue was immediately placed into 50-ml conical tubes, filled with sterile RPMI media, and stored for 2–6 hours at 4°C before processing. This short timeframe ensured maximal cell survival. Single-cell suspensions were prepared by mincing tissue into small pieces with scissors and incubating for 1 hour with 2 mg · ml^{-1} collagenase D (Roche) and 20 mg · ml^{-1} DNase I (Roche) in sterile RPMI at 37°C with shaking at 200 rpm.

Digested tissue was then pressed through 70-μm cell strainers (BD Falcon). Samples were underlaid with Ficoll-Paque (GE Healthcare) and centrifuged at 2,000 rpm for 20 minutes at room temperature with the brake off. The interface layer was removed with a pipette. Samples usually did not contain red blood cells. If red blood cells did remain, cells were lysed with ACK buffer (Gibco). For sample storage, cells were stored in 1 ml of freezing media (90% fetal bovine serum, 10% DMSO) and frozen in a Nalgene Mr. Frosty container (Thermo Scientific) at −80°C. At 48–96 hours after freezing, cryovials were moved to liquid nitrogen for long-term storage (maximum of 4 yr) until analysis.

Flow Cytometry

Samples were treated as a single cohort to ensure maximal consistency. All samples were thawed, stained with flurochrome-conjugated antibodies, and acquired over consecutive days on one flow cytometer analyzer with identical laser voltage and compensation settings maintained each day

of acquisition. No significant laser drift was observed between days of acquisition.

Sample cryovials were quick-thawed in a 37°C incubator. Each sample was washed with sterile RPMI media, passed through a 70-μm filter (Miltenyi Biosciences), and centrifuged at 1,600 rpm for 5 minutes at 4°C. Cell pellets were resuspended in FACS Buffer (2% fetal bovine serum in phosphate-buffered saline). Single-cell suspensions were stained with the following monoclonal fluorescently conjugated antibodies for 1 hour at 4°C in the dark. Antibodies were from eBioscience and used at 1:100 dilution unless specified otherwise. Viability dye was Live/Dead Fixable Aqua, dilution 1:600 (Invitrogen). Anti-human CD3e (OKT3), CD4 (OKT4), CD5 (UCHT2), CD14 (61D3), CD16 (CB16), CD19 (HIB19), CD56 (B159), CD25 (BC96), CD45 (HI30), CD127 (dilution 1:50; eBioRDR5), CRTH2 (BM16, dilution 1:50; BD Biosciences), and FcεR1α (AER-37) were used. After surface staining, samples were fixed for 30 minutes with 2% paraformaldehyde (freshly diluted in phosphate-buffered saline from 16%

paraformaldehyde) and resuspended in FACS Buffer. Immediately before acquisition, samples were filtered through sterile 40-μm filter-capped 5-ml tubes (BD Falcon). Samples were acquired in their entirety on a custom configuration five-laser BD Fortessa flow cytometer (BD Biosciences) and analyzed using FlowJo software (v9.2; Tree Star).

Exclusion Criteria and Statistical Analysis

The following exclusion criteria were applied. Any samples with viability of 30% or lower (determined by flow cytometric staining of viability dye [Live/Dead Fixable Aqua; Invitrogen]) were excluded from all analyses. Any samples with fewer than 50 total ILCs (determined as the number of live, $CD45^+$, lineage negative [Lin^-], $CD127^+$ cells) were excluded for ILC analysis but were used for NK or CD4 T–cell analyses. Depending on the cell type analyzed, group sizes ranged from 3 to 18. Exact number of transplant recipients analyzed (n) is specified in each legend. Only matched pre- and postreperfusion allograft biopsies from the same donor were used for all analyses. If either the pre- or the postreperfusion biopsy met exclusion criteria as defined previously here, then both biopsies from that subject were excluded. Donor, recipient, and perioperative demographics were compared using Student's t test or chi-square analysis, as appropriate. The impact of allograft reperfusion on ILC population numbers was evaluated using the Wilcoxon matched-pairs signed-rank test to account for repeated measures within an individual. The association of changes in ILC levels with allograft reperfusion and PGD were evaluated using rank sum tests given the small sample sizes and nonnormality of the data. We also evaluated changes in ILC population levels within the two most common transplant indications, COPD and ILD. A P value less than 0.05 was considered statistically significant. STATA version 14.2 was used for all analyses (STATA Corp.), and Prism 7 (GraphPad Software) was used for generating graphs.

Results

To examine whether changes in donor-derived ILC populations correlate with incidence of PGD after lung transplantation, we performed a single-center cohort study

Table 1. Subject Demographics of Lung Transplant Patients as Defined by PGD Grade 3 Status

Covariate	PGD ($n = l$)	Non-PGD ($n = 11$)	P Value
Donor variables			
Sex, M, n (%)	4 (57)	7 (64)	0.8
Age, mean, yr	33.4	38.6	0.5
Race, n (%)			0.3
White	5 (71)	10 (91)	
African American	2 (29)	1 (9)	
Any smoking, yes, n (%)	4 (57)	8 (73)	0.5
Recipient variables			
Sex, M, n (%)	4 (57)	7 (64)	0.8
Age, mean, yr	61.3	61.3	0.9
BMI, mean	26.1	25.8	0.9
Pulmonary diagnosis, n (%)			0.5
Chronic obstructive pulmonary disease	3 (43)	6 (55)	
Interstitial lung disease	3 (43)	5 (45)	
Chronic rejection	1 (14)	0 (0)	
PASP, mean	33.3	30.5	0.6
Race, n (%)			0.02
White	4 (57)	11 (100)	
African American	3 (43)	0	
Operative variables			
Ischemic time, min, mean	367	271	0.1
Transplant type, single, n (%)	4 (57)	7 (64)	0.8
Cardiopulmonary bypass use, yes, n (%)	3 (43)	5 (45)	0.9

Definition of abbreviations: BMI = body mass index; PASP = pulmonary artery systolic pressure; PGD = primary graft dysfunction.
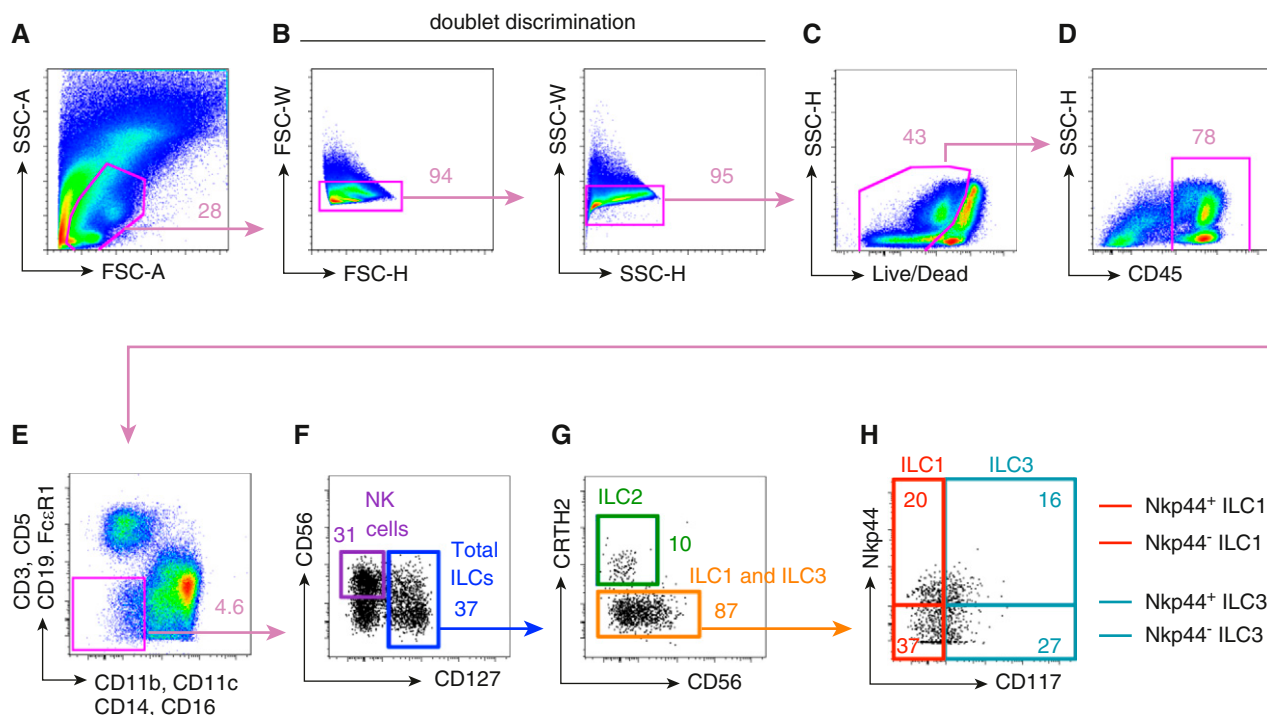Percentages may not exactly equal 100% because of rounding.

Figure 1. Flow cytometric identification of innate lymphocyte subsets in human lung tissue allograft biopsies. Shown is a flow cytometric analysis of a representative lung allograft biopsy. Total events were gated by (*A*) forward and side scatter gating (FSC and SSC), (*B*) doublet discrimination for single cells, (*C*) live cells, and (*D*) hematopoietic cells (CD45). (*E*) A combination of lineage marker antibodies (CD3, CD5, Cd19 FcεR1, CD11b, CD11c, CD14, and CD16) identified the lineage negative fraction (pink box). (*F*) Natural killer (NK) cells were identified as CD56$^+$CD127$^-$ (purple box). (*F*) Total innate lymphoid cells (ILCs) were identified as lineage negative CD127$^+$ (blue box) and then split into ILC1, ILC2, and ILC3 subsets. (*G*) ILC2s were defined as CRTH2$^+$ (green box). (*H*) ILC1s were defined as CRTH2$^-$CD117$^+$NKp44$^{+/-}$ (red box). (*H*) ILC3s were defined as CRTH2$^-$CD117$^+$NKp44$^{+/-}$ (teal box). Data are representative of *n* = 18 lung transplant recipient patients (36 total samples; 1 prereperfusion and 1 postreperfusion allograft biopsy taken for each lung transplant recipient).

of lung transplantation patients with small surgical biopsies of donor tissue taken before, and immediately after, allograft reperfusion (*see* Figure E1 for flowchart of patient enrollment). The incidence of grade 3 PGD in this cohort was 38.9% (*n* = 7/18). The overall demographics of the cohort are presented in Table 1. The proportion of African American recipients was significantly higher in the patients with PGD compared with those without PGD (*P* = 0.02). There were no other significant differences noted between the PGD versus non-PGD groups in donor, recipient, or intraoperative characteristics (Tables 1 and E1).

Compared with conventional lymphocytes and myeloid cells, ILCs are a rare cellular population in the respiratory tract, and extreme care must be taken to ensure stringent flow cytometric staining and analysis, especially in small-sized samples. To ensure scientific rigor, we took several approaches. First, to achieve maximal cell viability, we designed the study

to allow for a minimal time lapse between surgical biopsy removal and subsequent tissue processing (maximum 6 h from time of removal to start of tissue digestion). Second, we designed a 16-antibody flow cytometric staining panel with multiple negative or positive cell surface markers to allow for detailed single-cell resolution of all known ILC subsets without contamination of other immune cell populations (Figure 1 and Figure E2). Third, we imposed strict exclusion criteria that ensured all biopsies analyzed had met viability and ILC yield thresholds (*see* METHODS). Taken together, these approaches ensured generation of scientifically robust data from these small-sized, minimally invasive biopsies from the donor allograft.

To characterize the immune cell composition within the allograft, the surgically removed biopsy tissue was enzymatically digested, hematopoietic cells were enriched using Ficoll purification, and single-cell suspensions were frozen

until the full cohort of samples was collected (collection spanned 12 mo). Samples were then thawed and stained with flurochrome-conjugated antibodies for phenotypic characterization by flow cytometry.

Immune cell populations were phenotypically characterized using the following gating strategy. Total events were first subjected to size discrimination by forward and side scatter gating to focus on lymphocyte and myeloid cells while excluding large-sized epithelial or stromal cells (Figure 1A). Next, we employed doublet discrimination by forward versus side scatter height and width to ensure only single cells would be analyzed (Figure 1B). Use of a viability dye excluded dead cells (Figure 1C), and a hematopoietic marker, CD45 (Figure 1D), further eliminated any residual epithelial or stromal cells from analysis. Cells in the ILC family are defined as Lin$^-$, lacking expression of classical surface markers associated with granulocytes, dendritic cells, macrophages,
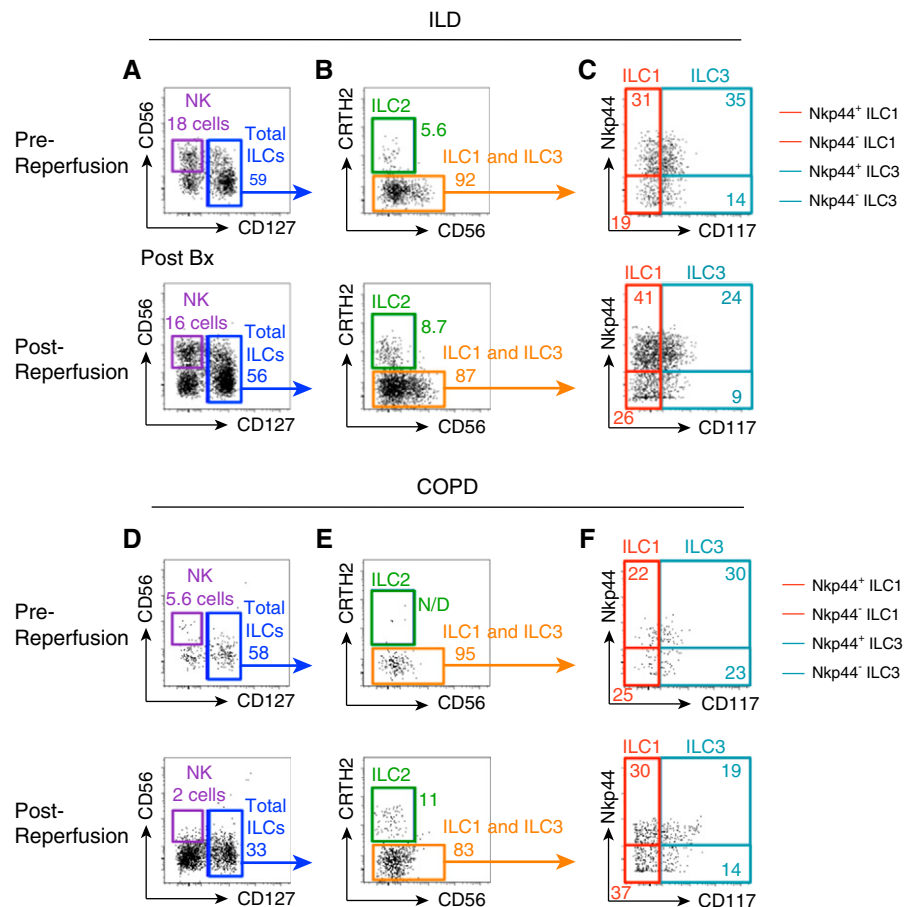
Figure 2. Single-cell resolution of innate immune cell subsets in pre- and postreperfusion lung allograft biopsies in transplant patients. (A–F) Representative flow cytometric gating of innate lymphoid cell (ILC) subsets from lung allograft biopsies taken before or after reperfusion from patients diagnosed with interstitial lung disease (ILD) (A–C) or chronic obstructive pulmonary disease (COPD) (D–F). (A and D) Natural killer (NK) cells were identified as $CD56^+CD127^-$ (purple box). (A and D) Total ILCs were identified as lineage negative $CD127^+$ (blue box), and then split into ILC1, ILC2, and ILC3 subsets. (B and E) ILC2s were defined as $CRTH2^+$ (green box). (C and F) ILC1s were defined as $CRTH2^-CD117^+NKp44^{+/-}$ (red box). (C and F) ILC3s were defined as $CRTH2^-CD117^+NKp44^{+/-}$ (teal box). Data are representative of one prereperfusion and one postreperfusion allograft biopsy taken for each lung transplant recipient; $n = 15$ recipients. N/D = not detected.

and conventional B and T lymphocytes (17). Therefore, we next used a combination of lineage marker antibodies (CD3, CD5, CD19, FcεR1, CD11b, CD11c, CD14, and CD16) to identify the Lin⁻ fraction where the ILCs reside (Figure 1E, pink box). Total ILCs were then positively identified by expression of CD127 (IL-7Rα; Figure 1F, blue box). Classical NK cells were identified by $CD56^+$ $CD127^-$ (Figure 1F, purple box). To divide the $CD127^+$ total ILC population into the three main ILC subsets, first the ILC2 population was identified by CRTH2 expression (23, 37–39) (Figure 1G, green box). ILC1s were then defined by lack of expression for

CRTH2 and CD117 (c-kit), and a portion expressed the cytoxicity-activating receptor, NKp44 (Figure 1H, red box) (19, 39–41). Lastly, ILC3s were defined as $CRTH2^-$ $CD117^+$ cells, and a portion expressed NKp44 (39–42) (Figure 1H, teal box).

Representative flow cytometric analysis of pre- and postreperfusion biopsies from two patients diagnosed with either of the two primary indications for lung transplantation (ILD [Figure 2A] or COPD [Figure 2B]) revealed that NK cells and all three ILC subsets could be identified both before and after graft reperfusion. Interestingly, analysis of these two representative patients suggested

substantial variability in the cell number, subset frequencies, and activation status (determined by NKp44 expression) of the ILC1, ILC2, and ILC3 populations before and after graft reperfusion (Figure 2). Notably, although there was substantial variation in the total ILC yield across all donor allografts (events ranged from 68 to 1,884), there was no significant difference between patients with ILD and those with COPD (data not shown), suggesting that variation in cell yield may be an inherent feature of using small-sized allograft biopsies and appears unrelated to the disease diagnosis of the transplant recipient.

Using this high-resolution flow cytometric gating strategy, we quantified the frequencies of immune cell populations in 18 patients to evaluate the impact of allograft reperfusion. Interestingly, although frequencies of conventional $CD4^+$ T cells did not appear to change after graft reperfusion in either patients with ILD or those with COPD (Figures 3A–3C), we observed a significant decrease in $CD56^+$ NK cells after graft reperfusion (0.3 vs. 0.14, $P = 0.009$; Figures 3D–3F). Collectively these results suggest that the effects of allograft reperfusion may more strongly influence the innate immune system rather than the adaptive immune compartment.

Next, we evaluated the differences in ILC subset composition pre- and posttransplant to determine the effect of allograft reperfusion. Analysis of the frequency of total ILCs (Lin⁻ $CD127^+$) as a proportion of all $CD45^+$ hematopoietic cells revealed an apparent, but non–statistically significant, reduction in ILCs (Figure 4A) after reperfusion that was observed in both transplant recipients with ILD (Figure 4B) and those with COPD (Figure 4C). Particularly in transplant recipients with ILD, the decrease in ILC frequency after graft reperfusion appeared to be largely driven by a reduction in the ILC2 subset (Figures 4D and 4E), which was not observed in patients with COPD (Figure 4F). Next, to determine whether the other ILC subsets were affected during graft reperfusion, we quantified the frequencies of ILC1 and ILC3 populations and evaluated their activation status by expression of the NCR (natural cytotoxicity receptor), NKp44. There was substantial variability in the proportion of both NCR^+ and NCR^- ILC1s across all patients
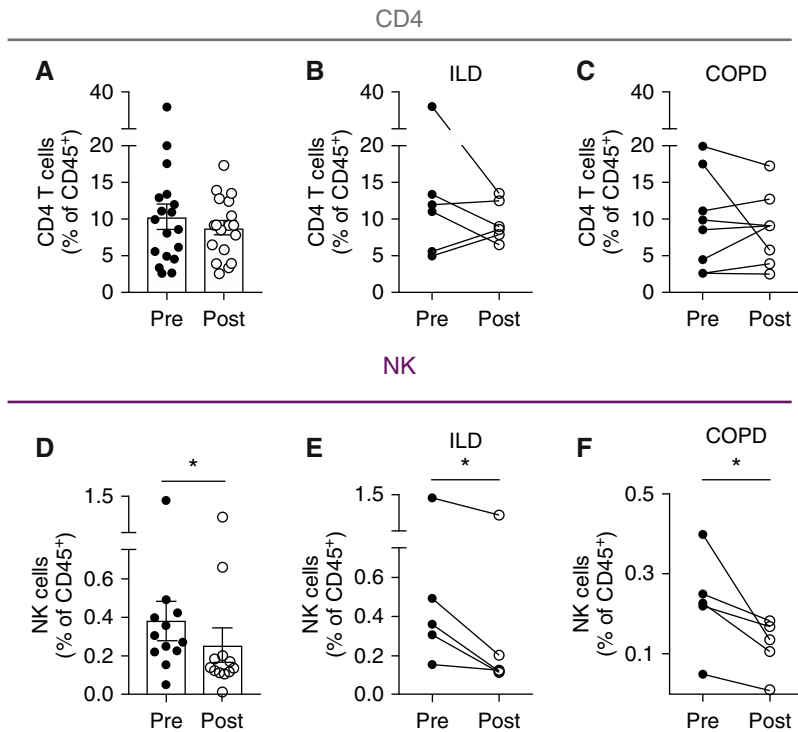
CD4

NK

Figure 3. Graft reperfusion is associated with selective decrease in donor natural killer (NK) cells without affecting CD4 T-cell responses. (A–C) Flow cytometric analysis of total $CD4^+$ T-cell frequencies (live, $CD45^+CD3^+CD4^+$) in pre- and postreperfusion allograft biopsies (A; $n = 18$) from interstitial lung disease (ILD) (B; $n = 6$) or chronic obstructive pulmonary disease (COPD) (C; $n = 8$) lung transplant recipients. (D–F) Flow cytometric analysis of total NK cell frequencies (live, $CD45^+$ lineage negative $CD127^-CD56^+$) in pre- and postreperfusion allograft biopsies (D; $n = 12$) from ILD (E; $n = 5$) or COPD (F; $n = 5$) lung transplant recipients. *$P < 0.05$.

Discussion

In this cohort study, we demonstrate, for the first time, that lung-resident ILCs can be isolated from small-sized biopsies of the donor allograft and that high-resolution flow cytometric analysis can reveal dynamic ILC population changes after graft reperfusion. Notably, we found that alterations in the relative abundance of selective ILC1 and ILC2 subsets correlate with PGD development after transplantation. These findings provide preliminary evidence for novel immune pathways that may be effective targets for improved therapeutic strategies to prevent PGD development in lung transplant recipients.

ILCs are a rare immune cell family, and technological limitations have been a significant hurdle in examining the potential involvement of these cells in human disease. Here, for the first time, we demonstrate the feasibility of live cell isolation and high-resolution flow cytometric phenotyping of ILC populations from small biopsy specimens. Previously, studies correlating changes in ILC populations with adult human lung diseases have been based almost exclusively on blood, and only rarely on BAL fluid or sputum (19, 20, 22–24, 43). Typically, lung tissue is not examined, raising concerns that conclusions drawn may not be biologically relevant to the immunological changes occurring at the tissue site of inflammation. Furthermore, many of these previous studies had very few ILCs recorded on flow plots or used flow cytometric gating strategies that potentially include T-cell contamination (39, 43–48). In addition, although our group has previously identified robust numbers of ILCs in tissue samples from previously healthy lung donors (32) and those diagnosed with COPD or idiopathic pulmonary disease (49), those specimens were large-sized tissue explants. It has long been assumed by the research community that the rarity of ILCs precludes the ability to study ILC dynamics in small-sized tissue samples. Our success here represents a significant technological advance that should serve to encourage other groups to examine tissue-resident ILCs from small biopsy samples in future studies. Intriguingly, it should be noted that we did not isolate equal numbers of all ILC subsets from every allograft. This variability may

(Figures 4G and 4J), and there appeared to be no significant effect of graft reperfusion on cell frequencies in transplant recipients with either ILD (Figures 4H and 4I) or COPD (Figures 4K and 4L). Furthermore, although examination of ILC3s revealed no statistically significant impact on the NCR^+ subset in either patients with ILD or those with COPD (Figures 4M–4O), NCR^- ILC3 frequencies increased slightly after reperfusion (Figure 4P), with this change largely restricted to patients with ILD (Figure 4Q), but not patients with COPD (Figure 4R). Collectively, these results suggest that reperfusion may selectively alter the subset composition of donor ILCs within the graft.

We next assessed whether there is an association between changes in ILC populations and the development of PGD after transplantation. Although the rarity of ILCs limited the total number of allografts that could be examined, and this varied by ILC subset, we were able to identify patients with PGD ($n = 3–5$) and patients without

PGD ($n = 3–11$) that could be assessed for changes in ILC population dynamics. Notably, the proportion of NCR^- ILC1s was higher in the prereperfusion biopsies of patients without PGD compared with those with PGD (52.85 vs. 24.75; $P = 0.01$; Figure 5A). However, we did not observe significant changes in the proportion of NCR^+ ILC1s, nor were there alterations in the frequencies of NCR^- and NCR^+ ILC3s (data not shown). Strikingly, examination of ILC2 frequencies revealed a significant reduction in ILC2s after graft reperfusion in patients with PGD (6.7 vs. 2.3; Figure 5B), suggesting that ILC2 frequencies may be associated with protection from PGD. Supporting this, patients without PGD exhibited moderately increased ILC2 frequencies after graft reperfusion (3.3 vs. 4.9) (Figure 5B). Taken together, these results suggest that changes in the subset composition of donor-derived ILCs within the allograft, particularly the presence of ILC2s, may be linked to the incidence of PGD.
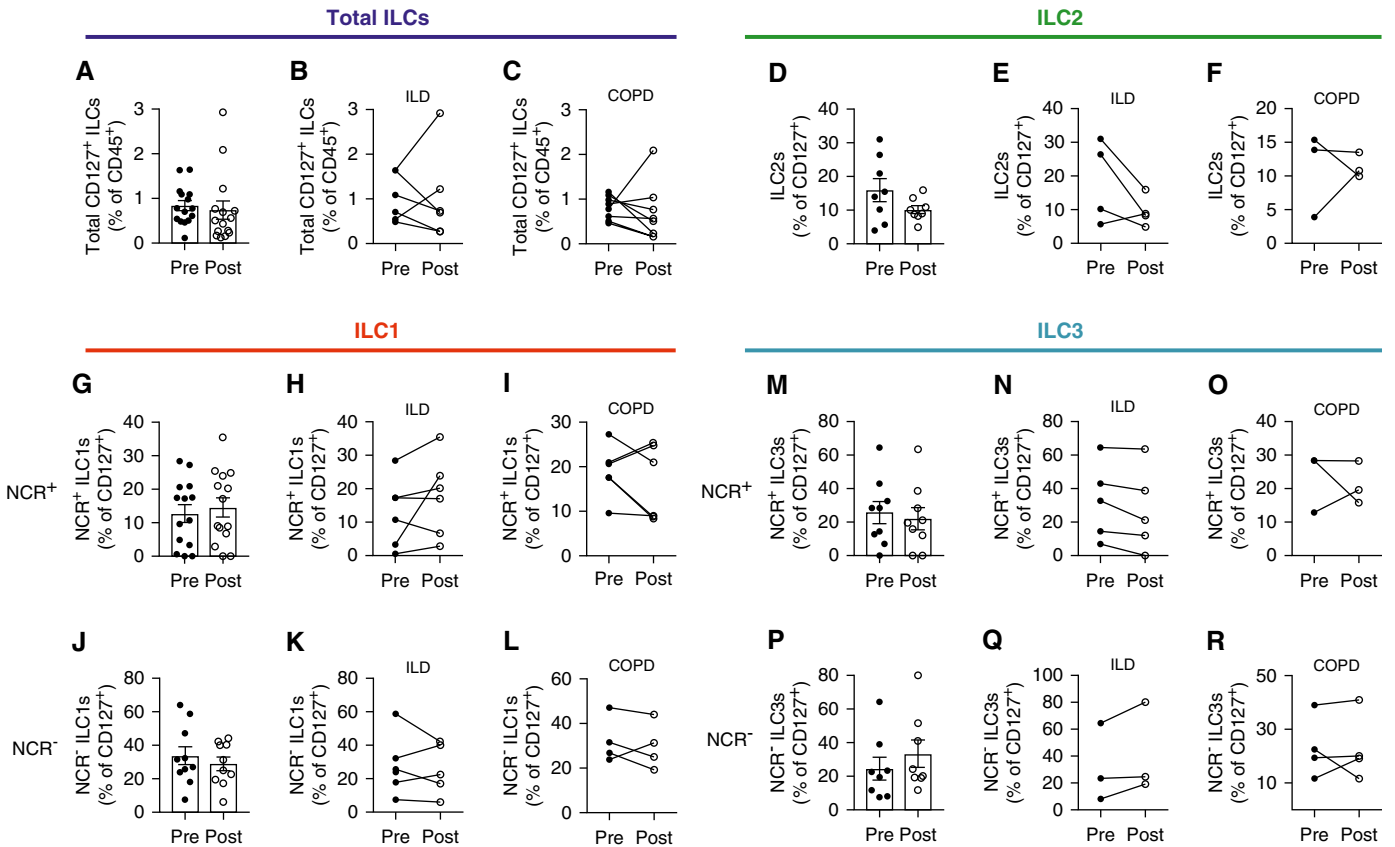
Figure 4. Distribution of multiple innate lymphoid cell (ILC) subsets fluctuates after donor graft reperfusion. (*A–C*) Flow cytometric analysis of total ILC frequencies (live, CD45$^+$ lineage negative [Lin$^-$] CD127$^-$) in pre- and postreperfusion allograft biopsies (*A*; $n = 15$) from lung transplant recipients with interstitial lung disease (ILD) (*B*; $n = 6$) or chronic obstructive pulmonary disease (COPD) (*C*; $n = 8$). (*D–F*) Flow cytometric analysis of total ILC2 frequencies (live, CD45$^+$Lin$^-$CD127$^-$CD56$^-$CRTH2$^+$) in pre- and postreperfusion allograft biopsies (*D*; $n = 8$) from ILD (*E*; $n = 4$) or COPD (*F*; $n = 3$) lung transplant recipients. (*G–I*) Flow cytometric analysis of total natural killer (NK) p44$^+$ILC1 frequencies (live, CD45$^+$Lin$^-$CD127$^-$CRTH2$^-$CD56$^{+/-}$CD117$^-$NKp44$^+$) in pre- and postreperfusion allograft biopsies (*G*; $n = 14$) from lung transplant recipients with ILD (*H*; $n = 6$) or COPD (*I*; $n = 5$). (*J–L*) Flow cytometric analysis of total NKp44$^-$ILC1 frequencies (live, CD45$^+$Lin$^-$CD127$^-$CRTH2$^-$CD56$^{+/-}$CD117$^-$NKp44$^-$) in pre- and postreperfusion allograft biopsies (*J*; $n = 10$) from lung transplant recipients with ILD (*K*; $n = 6$) or COPD (*L*; $n = 4$). (*M–O*) Flow cytometric analysis of total NKp44$^+$ILC3 frequencies (live, CD45$^+$Lin$^-$CD127$^-$CRTH2$^-$CD56$^{+/-}$CD117$^+$NKp44$^+$) in pre- and postreperfusion allograft biopsies (*M*; $n = 9$) from lung transplant recipients with ILD (*N*; $n = 5$) or COPD (*O*; $n = 3$). (*P–R*) Flow cytometric analysis of total NKp44$^-$ILC3 frequencies (live, CD45$^+$Lin$^-$CD127$^-$CRTH2$^-$CD56$^{+/-}$CD117$^+$NKp44$^-$) in pre- and postreperfusion allograft biopsies (*P*; $n = 8$) from lung transplant recipients with ILD (*Q*; $n = 3$) or COPD (*R*; $n = 4$). NCR = natural cytotoxicity receptor.

simply represent the technical limitations of working with such small samples; however, it may also indicate a selective loss of distinct ILC subpopulations within the transplanted lung that potentially correlates with important clinical outcomes, including, but not limited to, PGD.

The unique design of this cohort study allowed us to be the first to track dynamic changes in ILC subset composition by examining donor grafts before and immediately after reperfusion. We identified marked changes in certain populations of innate cells in the setting of allograft reperfusion, notably the steep decline of NK cells and ILC2s in patients with ILD. Although it is possible that circulating cells

may contribute to these population changes, ILC2s are rare in blood by volume, and we observed very little blood in the biopsies, suggesting that the fluctuating NK and ILC frequencies after reperfusion are indicative of lung tissue–resident populations and not circulating cells. The rapid changes we observed in innate cells, but not adaptive CD4$^+$ T cells, highlight how highly sensitive these particular donor immune cells are to the tissue environment after transplantation.

PGD remains the primary cause of morbidity and mortality for lung transplant patients, and there is an urgent need to identify new therapeutic targets. Here, we sought to address whether we could identify

changes in distinct donor-derived ILC populations associated with incidence of graft dysfunction after transplantation. Notably, the proportion of ILC1s lacking NKp44 expression (NCR$^-$) was higher in the prereperfusion biopsies of patients without PGD compared with those with PGD, suggesting that the presence of this "less active" ILC1 population may be associated with protection from ischemia–reperfusion–induced graft dysfunction. Relatively little is known about the role of ILC1s in the respiratory tract, but recent studies suggest that blood ILC1 frequencies correlate with severity of COPD (19). In addition, studies of inflamed intestinal tissue suggest that NCR$^-$ ILC1s
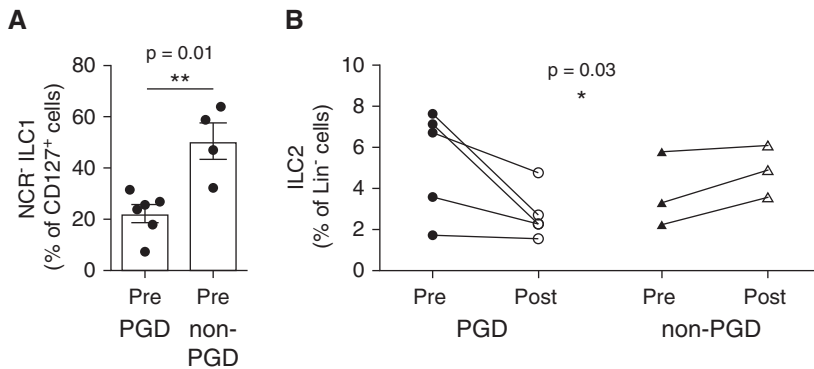
Figure 5. Incidence of pulmonary graft dysfunction is associated with reduced frequency of group 1 and group 2 innate lymphoid cells (ILCs). (*A*) Flow cytometric analysis of natural killer p44−ILC1 frequencies (live, CD45+ lineage negative [Lin−] CD127−CRTH2−CD56+/−CD117−natural killer p44−) in prereperfusion allograft biopsies from lung transplant recipients with primary graft dysfunction (PGD) (*n* = 5) or without PGD (*n* = 4). (*B*) Flow cytometric analysis of ILC2 frequencies (live, CD45+Lin−CD127−CD56−CRTH2+) in pre- and postreperfusion allograft biopsies from lung transplant recipients with PGD (*n* = 5) or without PGD (*n* = 3). *P < 0.05 and **P < 0.01. NCR = natural cytotoxicity receptor.

are a heterogeneous population capable of producing IFNγ (41, 50) and may in fact contain NK/ILC progenitors (39). Further studies are needed to determine how lung-resident ILC1s may contribute to PGD development. In contrast, the potential role for ILC2s in lung tissue injury and repair is more apparent. Murine models have demonstrated ILC2s are essential for regulating the balance between driving pathologic inflammation (via IL-5 and IL-13) in response to allergens (18, 26–28, 30, 31) or promoting host-protective airway repair after severe lung injury (via amphiregulin–epidermal growth factor receptor interactions) (32). Here, we identified dynamic changes in ILC2 frequencies before and after graft reperfusion that correlated with PGD status. The elevated ILC2s observed in patients without PGD that are substantially diminished after graft reperfusion in patients with PGD suggest that reduced frequency of these "tissue-protective" ILC2s may potentially impair the ability of donor

lungs to repair and restore tissue homeostasis after transplantation.

Intriguingly, all patients with PGD grade 3 at 72 hours also had grade 3 PGD present within the first 24 hours. Furthermore, all patients except for one had grade 3 PGD on Postoperative Day 0. Given these data, it is possible that the rapid alterations observed in ILC frequency before and after transplantation may have both immediate and longer-term effects as PGD develops. Although it may seem surprising that such early alterations in ILC populations could have lasting consequences, mechanistic animal studies have shown that lung ILC2s in particular serve dual roles, both as rapid "first responders" as well as key "gatekeeper" cells that initiate the broader immunological cascade-controlling processes of tissue inflammation versus repair. Cytokines and growth factors produced by ILC2s can have immediate, localized effects in the tissue by driving inflammatory cell recruitment (18, 26–28, 31), but they can

also cause longer-term consequences by initiating adaptive immune responses (30) or by promoting morphological changes in lung tissue remodeling (32). Additional larger cohort studies will be needed to determine the precise mechanisms by which the dysregulated ILC frequencies observed in the graft may be contributing to development of PGD. In addition, the upstream factors that regulate ILC responses in the lung tissue during transplantation are unknown. In this study, we did not observe significant differences between the PGD versus non-PGD groups in donor, recipient, or intraoperative characteristics. There was a trend toward increased ischemia time in patients that went on to develop PGD, but larger cohort studies have not found evidence to support ischemia time as a risk determinant for PGD (3). The question of whether lung ILC responses during transplantation are influenced by donor, recipient, or intraoperative characteristics remains an open area for future investigation.

In conclusion, this single-center cohort study provides preliminary evidence to support the hypothesis that changing ILC dynamics, particularly the loss and gain within the ILC2 subset, may be associated with incidence of PGD. Further analysis in a larger cohort will be necessary to examine whether these cells play a mechanistic role in lung injury or repair during graft rejection. The ability to therapeutically manipulate ILC2s and their production of tissue-protective growth factors, such as amphiregulin, may be a useful approach for aiding in maintenance of tissue homeostasis and protection against graft injury. ∎

References

1. Christie JD, Bavaria JE, Palevsky HI, Litzky L, Blumenthal NP, Kaiser LR, *et al*. Primary graft failure following lung transplantation. *Chest* 1998; 114:51–60.
2. Diamond JM, Arcasoy S, Kennedy CC, Eberlein M, Singer JP, Patterson GM, *et al*. Report of the International Society for Heart and Lung Transplantation Working Group on Primary Lung Graft Dysfunction, part II: epidemiology, risk factors, and outcomes—a 2016 Consensus Group statement of the International Society for Heart and Lung Transplantation. *J Heart Lung Transplant* 2017;36: 1104–1113.
3. Diamond JM, Lee JC, Kawut SM, Shah RJ, Localio AR, Bellamy SL, *et al*.; Lung Transplant Outcomes Group. Clinical risk factors for primary graft dysfunction after lung transplantation. *Am J Respir Crit Care Med* 2013;187:527–534.
4. Liu Y, Liu Y, Su L, Jiang SJ. Recipient-related clinical risk factors for primary graft dysfunction after lung transplantation: a systematic review and meta-analysis. *PLoS One* 2014;9: e92773.
5. Sharma AK, LaPar DJ, Stone ML, Zhao Y, Mehta CK, Kron IL, *et al*. NOX2 activation of natural killer T cells is blocked by the adenosine A2A receptor to inhibit lung ischemia–reperfusion injury. *Am J Respir Crit Care Med* 2016;193:988–999.

6. Fiser SM, Tribble CG, Long SM, Kaza AK, Cope JT, Laubach VE, *et al*. Lung transplant reperfusion injury involves pulmonary macrophages and circulating leukocytes in a biphasic response. *J Thorac Cardiovasc Surg* 2001;121: 1069–1075.

7. Eppinger MJ, Jones ML, Deeb GM, Bolling SF, Ward PA. Pattern of injury and the role of neutrophils in reperfusion injury of rat lung. *J Surg Res* 1995;58:713–718.

8. Naidu BV, Krishnadasan B, Farivar AS, Woolley SM, Thomas R, Van Rooijen N, *et al*. Early activation of the alveolar macrophage is critical to the development of lung ischemia–reperfusion injury. *J Thorac Cardiovasc Surg* 2003;126:200–207.

9. Yang Z, Sharma AK, Linden J, Kron IL, Laubach VE. CD4$^+$ T lymphocytes mediate acute pulmonary ischemia–reperfusion injury. *J Thorac Cardiovasc Surg* 2009;137:695–702. [Discussion, p. 702].

10. de Perrot M, Liu M, Waddell TK, Keshavjee S. Ischemia–reperfusion–induced lung injury. *Am J Respir Crit Care Med* 2003;167:490–511.

11. van der Kaaij NP, Kluin J, Haitsma JJ, den Bakker MA, Lambrecht BN, Lachmann B, *et al*. Ischemia of the lung causes extensive long-term pulmonary injury: an experimental study. *Respir Res* 2008;9: 28.

12. Johnston LK, Rims CR, Gill SE, McGuire JK, Manicone AM. Pulmonary macrophage subpopulations in the induction and resolution of acute lung injury. *Am J Respir Cell Mol Biol* 2012;47: 417–426.

13. Tait Wojno ED, Artis D. Emerging concepts and future challenges in innate lymphoid cell biology. *J Exp Med* 2016;213:2229–2248.

14. Cortez VS, Robinette ML, Colonna M. Innate lymphoid cells: new insights into function and development. *Curr Opin Immunol* 2015; 32:71–77.

15. Montaldo E, Vacca P, Vitale C, Moretta F, Locatelli F, Mingari MC, *et al*. Human innate lymphoid cells. *Immunol Lett* 2016;179:2–8.

16. Diefenbach A, Colonna M, Koyasu S. Development, differentiation, and diversity of innate lymphoid cells. *Immunity* 2014;41: 354–365.

17. Spits H, Artis D, Colonna M, Diefenbach A, Di Santo JP, Eberl G, *et al*. Innate lymphoid cells: a proposal for uniform nomenclature. *Nat Rev Immunol* 2013;13:145–149.

18. Artis D, Spits H. The biology of innate lymphoid cells. *Nature* 2015;517: 293–301.

19. Silver JS, Kearley J, Copenhaver AM, Sanden C, Mori M, Yu L, *et al*. Inflammatory triggers associated with exacerbations of COPD orchestrate plasticity of group 2 innate lymphoid cells in the lungs. *Nat Immunol* 2016;17:626–635.

20. Ohne Y, Silver JS, Thompson-Snipes L, Collet MA, Blanck JP, Cantarel BL, *et al*. IL-1 is a critical regulator of group 2 innate lymphoid cell function and plasticity. *Nat Immunol* 2016;17:646–655.

21. Everaere L, Ait-Yahia S, Molendi-Coste O, Vorng H, Quemener S, LeVu P, *et al*. Innate lymphoid cells contribute to allergic airway disease exacerbation by obesity. *J Allergy Clin Immunol* 2016;138: 1309–1318.e11.

22. Hams E, Armstrong ME, Barlow JL, Saunders SP, Schwartz C, Cooke G, *et al*. IL-25 and type 2 innate lymphoid cells induce pulmonary fibrosis. *Proc Natl Acad Sci USA* 2014;111: 367–372.

23. Bartemes KR, Kephart GM, Fox SJ, Kita H. Enhanced innate type 2 immune response in peripheral blood from patients with asthma. *J Allergy Clin Immunol* 2014;134:671–678.e4.

24. Barnig C, Cernadas M, Dutile S, Liu X, Perrella MA, Kazani S, *et al*. Lipoxin A4 regulates natural killer cell and type 2 innate lymphoid cell activation in asthma. *Sci Transl Med* 2013;5:174ra26.

25. Barlow JL, Peel S, Fox J, Panova V, Hardman CS, Camelo A, *et al*. IL-33 is more potent than IL-25 in provoking IL-13-producing nuocytes (type 2 innate lymphoid cells) and airway contraction. *J Allergy Clin Immunol* 2013;132:933–941.

26. Barlow JL, Bellosi A, Hardman CS, Drynan LF, Wong SH, Cruickshank JP, *et al*. Innate IL-13–producing nuocytes arise during allergic lung inflammation and contribute to airways hyperreactivity. *J Allergy Clin Immunol* 2012;129:191–198, e1–4.

27. Bartemes KR, Iijima K, Kobayashi T, Kephart GM, McKenzie AN, Kita H. IL-33-responsive lineage⁻ CD25$^+$ CD44(hi) lymphoid cells mediate innate type 2 immunity and allergic inflammation in the lungs. *J Immunol* 2012;188:1503–1513.

28. Kim HY, Chang YJ, Subramanian S, Lee HH, Albacker LA, Matangkasombut P, *et al*. Innate lymphoid cells responding to IL-33 mediate airway hyperreactivity independently of adaptive immunity. *J Allergy Clin Immunol* 2012;129:216–227.e1–6.

29. Chang YJ, Kim HY, Albacker LA, Baumgarth N, McKenzie AN, Smith DE, *et al*. Innate lymphoid cells mediate influenza-induced airway hyper-reactivity independently of adaptive immunity. *Nat Immunol* 2011;12:631–638.

30. Halim TY, Steer CA, Mathä L, Gold MJ, Martinez-Gonzalez I, McNagny KM, *et al*. Group 2 innate lymphoid cells are critical for the initiation of adaptive T helper 2 cell-mediated allergic lung inflammation. *Immunity* 2014;40:425–435.

31. Halim TY, Krauss RH, Sun AC, Takei F. Lung natural helper cells are a critical source of Th2 cell-type cytokines in protease allergen-induced airway inflammation. *Immunity* 2012;36: 451–463.

32. Monticelli LA, Sonnenberg GF, Abt MC, Alenghat T, Ziegler CG, Doering TA, *et al*. Innate lymphoid cells promote lung-tissue homeostasis after infection with influenza virus. *Nat Immunol* 2011; 12:1045–1054.

33. Diamond JM, Akimova T, Kazi A, Shah RJ, Cantu E, Feng R, *et al*.; Lung Transplant Outcomes Group. Genetic variation in the prostaglandin E2 pathway is associated with primary graft dysfunction. *Am J Respir Crit Care Med* 2014;189:567–575.

34. Christie JD, Carby M, Bag R, Corris P, Hertz M, Weill D; ISHLT Working Group on Primary Lung Graft Dysfunction. Report of the ISHLT Working Group on Primary Lung Graft Dysfunction part II: definition. A consensus statement of the International Society for Heart and Lung Transplantation. *J Heart Lung Transplant* 2005;24: 1454–1459.

35. Christie JD, Van Raemdonck D, de Perrot M, Barr M, Keshavjee S, Arcasoy S, *et al*.; ISHLT Working Group on Primary Lung Graft Dysfunction. Report of the ISHLT Working Group on Primary Lung Graft Dysfunction part I: introduction and methods. *J Heart Lung Transplant* 2005;24:1451–1453.

36. Snell GI, Yusen RD, Weill D, Strueber M, Garrity E, Reed A, *et al*. Report of the ISHLT Working Group on Primary Lung Graft Dysfunction, part I: definition and grading–a 2016 Consensus Group statement of the International Society for Heart and Lung Transplantation. *J Heart Lung Transplant* 2017;36:1097–1103.

37. Mjösberg JM, Trifari S, Crellin NK, Peters CP, van Drunen CM, Piet B, *et al*. Human IL-25– and IL-33–responsive type 2 innate lymphoid cells are defined by expression of CRTH2 and CD161. *Nat Immunol* 2011;12:1055–1062.

38. Mjösberg J, Bernink J, Golebski K, Karrich JJ, Peters CP, Blom B, *et al*. The transcription factor GATA3 is essential for the function of human type 2 innate lymphoid cells. *Immunity* 2012;37: 649–659.

39. Simoni Y, Fehlings M, Kløverpris HN, McGovern N, Koo SL, Loh CY, *et al*. Human innate lymphoid cell subsets possess tissue-type based heterogeneity in phenotype and frequency. *Immunity* 2017; 46:148–161.

40. Lim AI, Li Y, Lopez-Lastra S, Stadhouders R, Paul F, Casrouge A, *et al*. Systemic human ILC precursors provide a substrate for tissue ILC differentiation. *Cell* 2017;168:1086–1100.e10.

41. Bernink JH, Peters CP, Munneke M, te Velde AA, Meijer SL, Weijer K, *et al*. Human type 1 innate lymphoid cells accumulate in inflamed mucosal tissues. *Nat Immunol* 2013;14: 221–229.

42. Crellin NK, Trifari S, Kaplan CD, Cupedo T, Spits H. Human NKp44$^+$IL-22$^+$ cells and LTi-like cells constitute a stable RORC$^+$ lineage distinct from conventional natural killer cells. *J Exp Med* 2010;207:281–290.

43. De Grove KC, Provoost S, Verhamme FM, Bracke KR, Joos GF, Maes T, *et al*. Characterization and quantification of innate lymphoid cell subsets in human lung. *PLoS One* 2016;11: e0145961.

44. Burkhard SH, Mair F, Nussbaum K, Hasler S, Becher B. T cell contamination in flow cytometry gating approaches for analysis of innate lymphoid cells. *PLoS One* 2014;9:e94196.

45. Björklund AK, Forkel M, Picelli S, Konya V, Theorell J, Friberg D, *et al*. The heterogeneity of human CD127(+) innate lymphoid cells revealed by single-cell RNA sequencing. *Nat Immunol* 2016;17:451–460.

46. Sonnenberg GF. Transcriptionally defining ILC heterogeneity in humans. *Nat Immunol* 2016;17:351–352.

47. Nagasawa M, Germar K, Blom B, Spits H. Human CD5+ innate lymphoid cells are functionally immature and their development from CD34+ progenitor cells is regulated by Id2. *Front Immunol* 2017;8:1047.

48. Simoni Y, Newell EW. Toward meaningful definitions of innate-lymphoid-cell subsets. *Immunity* 2017;46:760–761.

49. Monticelli LA, Buck MD, Flamar AL, Saenz SA, Tait Wojno ED, Yudanin NA, *et al*. Arginase 1 is an innate lymphoid-cell–intrinsic metabolic checkpoint controlling type 2 inflammation. *Nat Immunol* 2016;17:656–665.

50. Klose CSN, Flach M, Möhle L, Rogell L, Hoyler T, Ebert K, *et al*. Differentiation of type 1 ILCs from a common progenitor to all helper-like innate lymphoid cell lineages. *Cell* 2014;157:340–356.